COMITATO NAZIONALE PER L'ENERGIA NUCLEARE
Laboratori Nazionali di Frascati

LNF - 66/30
6 Giugno 1966

S. Ferroni, V. Gracco, P. Lehmann, B. Merkel and C. Schaerf:

CHARGED PION PHOTOPRODUCTION ON LIGHT NUCLEI. -

(Nota interna : n. 324)

Servizio Documentazione
dei Laboratori Nazionali di Frascati del CNEN
Casella Postale 70 - Frascati (Roma)

Laboratori Nazionali di Frascati del CNEN
Servizio Documentazione

LNF-66/30

Nota Interna: n° 324
6 Giugno 1966

S. Ferroni(x), V. Gracco(x), P. Lehmann(x), B. Merkel(x) and C. Schaerf:
CHARGED PION PHOTOPRODUCTION ON LIGHT NUCLEI. -

ABSTRACT. -

The differential cross section for the photoproduction of charged pions on light nuclei has been measured for different values of the photon energy using the excitation curve method. Hydrogen, Lithium 6, Lithium 7 and Carbon have been studied. We found no correlation with the detailed structure of the final nuclei. The data seem consistent with a model where the nucleons are considered as independent emission centers and where reabsorption from the other nucleons in the nucleus is taken into account. This appears to be valid both for single and double pion photoproduction.

INTRODUCTION. -

Pion photoproduction on nuclei has been used for a long time as a source of information on nuclear structure. In particular the π^- / π^+ ratio has been found to be sensitive to the structure of the final nuclei.

This does not seem to be true if the energy transfer to the final nuclei is large. In addition, photoproduction of pion pairs is of interest for the possibility of coherent production. In this experiment the yield curve method has been used to obtain information on the photoproduction of pion pairs in light nuclei, using the Orsay Linear Electron Accelerator.

(x) - Ecole Normale Supérieure, Laboratoire de l'Accélérateur Linéaire Orsay, France.

EXPERIMENTAL APPARATUS. -

Electron Beam: The electrons accelerated by the Linac were momentum analysed using the three magnets system described in ref. 1. The setting of the analysing magnet was determined by a proton magnetic resonance probe situated in the magnet's gap, and by the voltage drop across a precision shunt in series with the magnet's windings. The energy defining slits were set to select a momentum band of $\pm$ 0.5% around the central value. The particles were then focused by a quadrupole doublet and entered the experimental area. The target was situated in a vacuum chamber, directly connected with the accelerator vacuum system, positioned on the axis of rotation of a magnetic spectrometer. After traversing the target the beam left the vacuum system and traversed three secondary emission monitors (SEM). The signal outputs of the monitors were connected to three current integrators (2) and continuously monitored during our data-taking period. The secondary emission monitors were calibrated against a Faraday cup for each value of the primary electron energy. The relative stability of two of our monitors was better than 1%. The third monitor had fluctuations of the order of a few percent and was not used to normalize our data.

The targets were mounted on a remotely controlled translating slide. To avoid possible sources of systematic errors measurements were made cycling the various targets at each primary electron energy.

Targets: Liquid Hydrogen, enriched Lithium 6, natural Lithium and high density graphite were used as targets. The measurements is hydrogen were performed with a different set-up and therefore are not directly comparable with the other measurements. In table I we have indicated the thickness and isotopic composition of the various solid targets used.

TABLE I

Target Name	Target Code	Thickness gr/cm^2	Radiation lengths	Isotopic Composition
Carbon	C	1.065	0.0246	98.89% C^{12}; 1.11% C^{13}
Natural Lithium	Li^N	0.955	0.0123	92.58% Li^7; 7.42% Li^6
Lithium 6	Li^6	0.166	0.0026	1.3% Li^7 ; 98.7% Li^6

Table I - contains the relevant information about the various solid targets used.

Detection apparatus: The pions produced in the target were momentum analysed using the double focusing zero dispersion magnetic spectrometer described in ref. 3. The energy defining slits of the spectrometer were set to accept a momentum interval of $\pm$ 1%. The pions transmitted by the magnet were detected by three scintillation counters in coincidence. The electronics consisted of 100 Mc, digital logic. Random coincidences were monitored by the delayed coincidence method, during all our data-taking runs.

EXPERIMENTAL RESULTS. -

The measurements have been performed at a constant angle and momentum for the pion, changing the primary electron energy. Pions were detected at 110° in the laboratory system with a momentum of 100 MeV/C.

Pions were produced in the reaction:

$$e + N \rightarrow e' + N' + \pi^-$$

The final electron was not detected. For this reason the double differential electroproduction cross section had to be integrated over all possible energies and directions for the final electron. This is equivalent to measuring the photoproduction cross section where the real photons are substituted by a virtual photon spectrum calculated as indicated in ref. 4. To normalize our data we have assumed a virtual radiator equivalent to 0.02 radiation lengths. To this we have added the real radiator contributed by the finite lengtn of the target.

The absolute value of the cross section has been estimated by a first order calculation of the optical properties of the magnet. It seems reasonable to associate to this calculation an error of 20%.

The result of the experiment is indicated in fig. 1, 2, 3 and 4.

The abscissa indicate the primary electron energy and the ordinate the pion yield per nucleus. This yield is given by:

$$Y(E) = \int_0^E \frac{d^2\sigma(k)}{d\Omega_\pi \, dT_\pi} \frac{f(E,k)}{k} dk \quad \text{microbarn/ster. MeV}$$

where E is the primary electron energy, k the energy of the gamma ray which photo-produces the pion, and f(E, k) is the energy spectrum of the Bremsstrahlung beam.

The straight lines have been obtained by a linear fit of the ex-

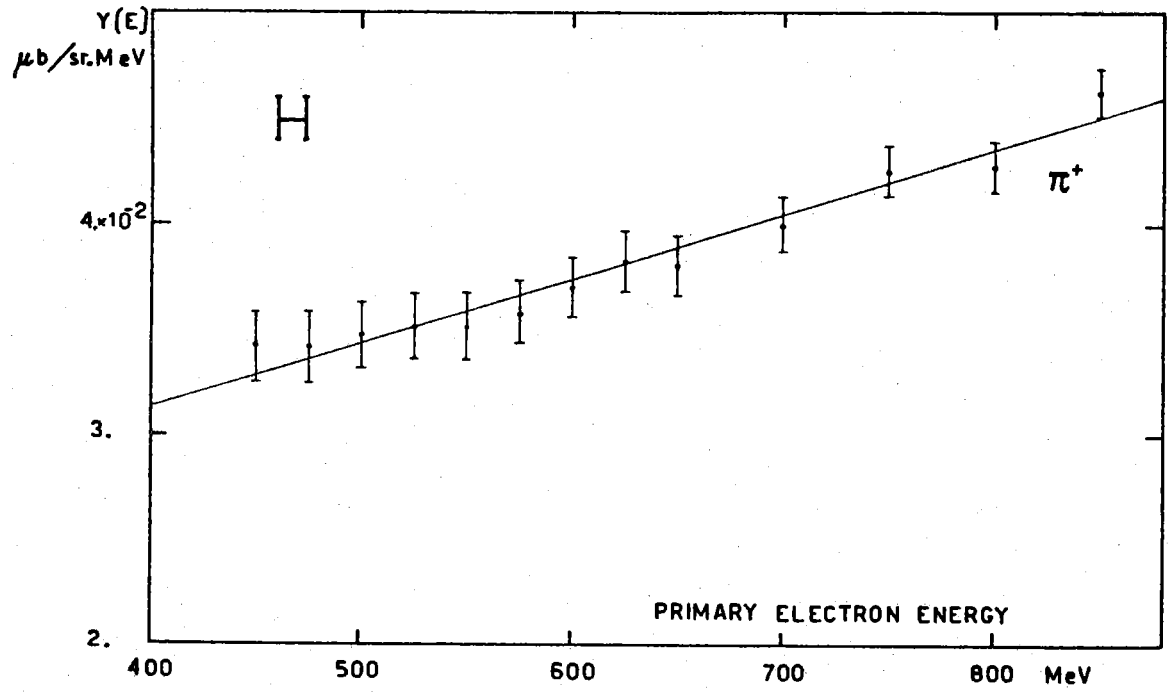

Fig. 1 indicates the yield curve obtained with the liquid hydrogen target.

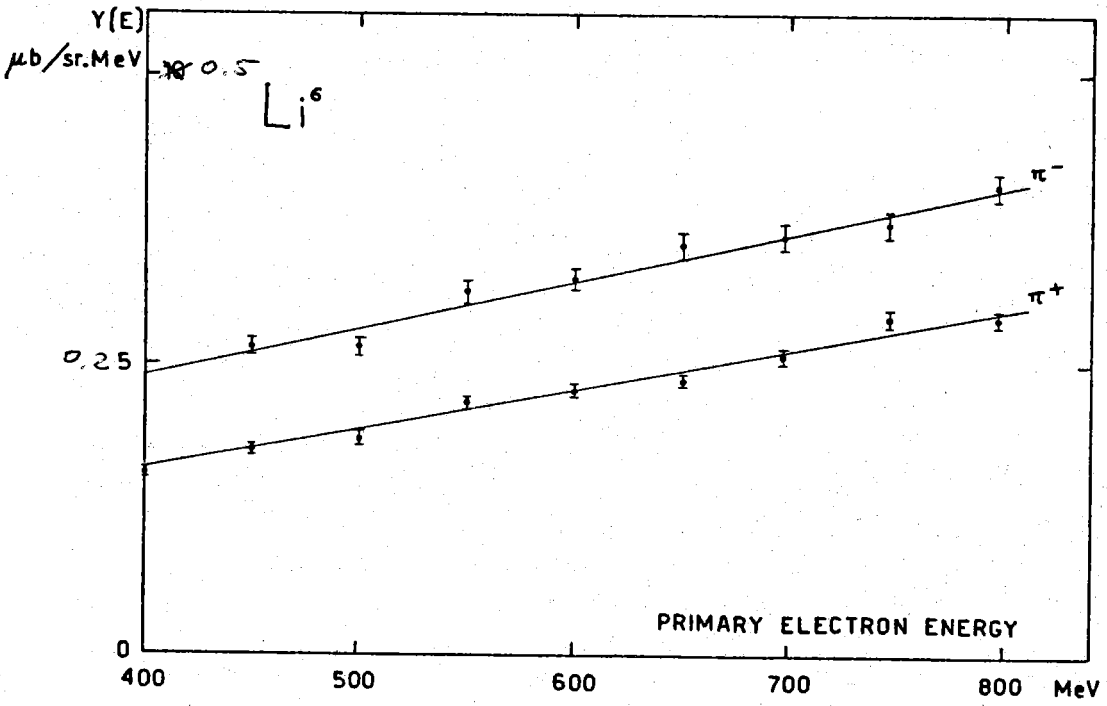

Fig. 2 indicates the yield curve for the Lithium 6 target.

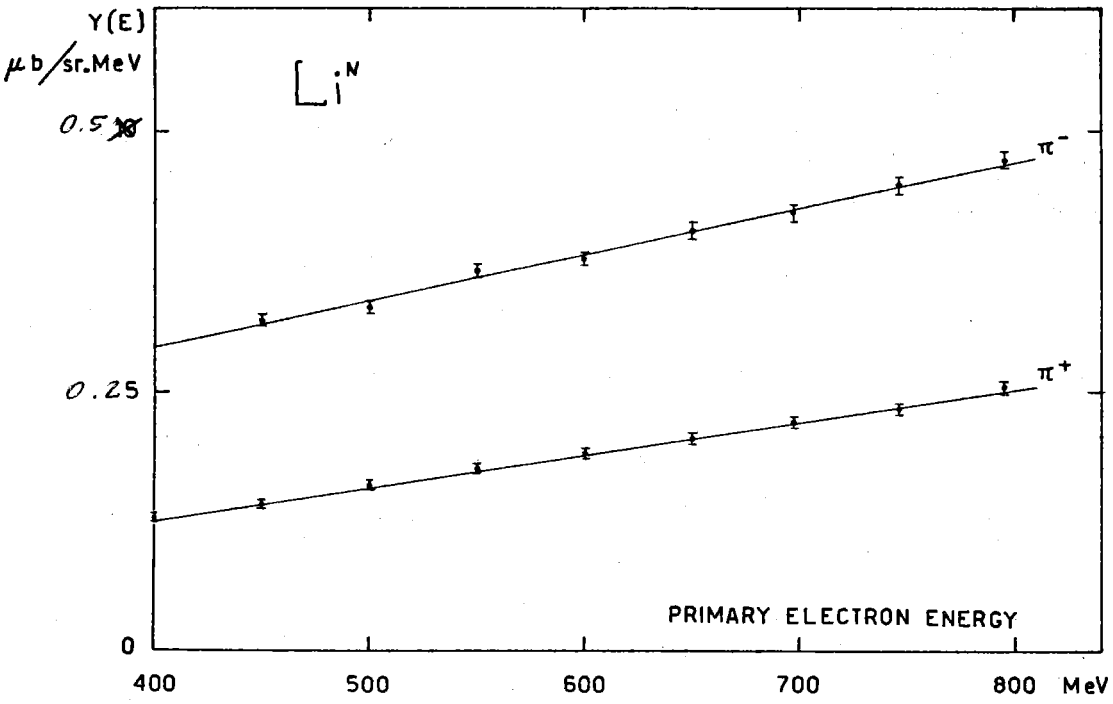

Fig. 3 indicates the yield curve for the Natural Lithium target.

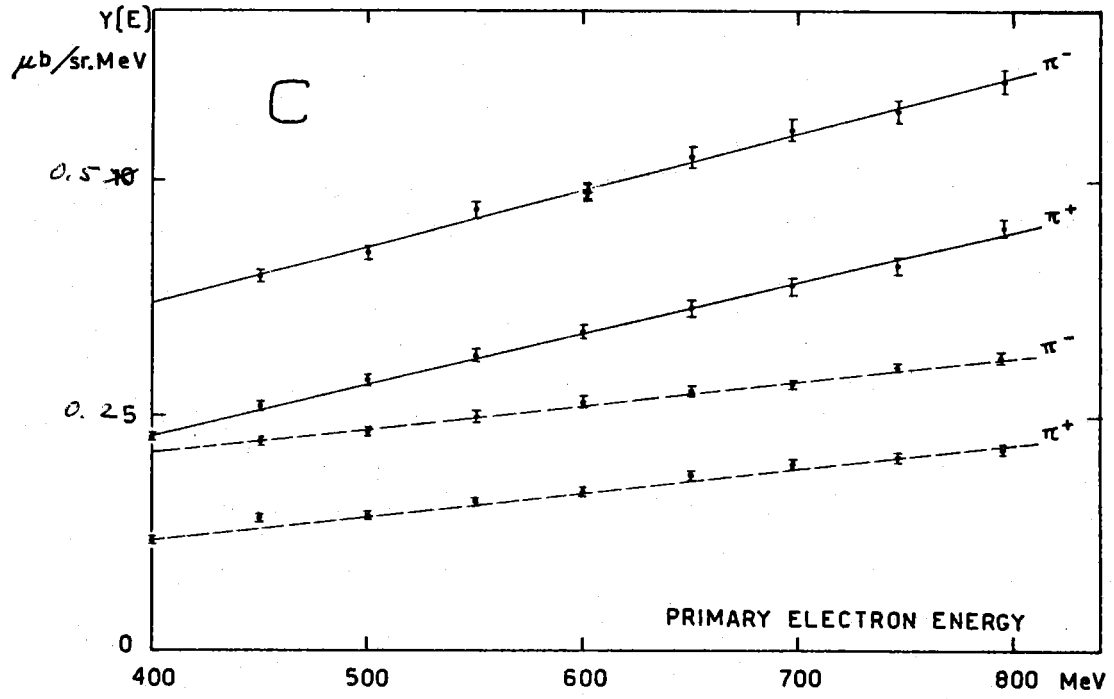

Fig. 4 indicates the yield curve for the Carbon target. The solid line is relevant to the points with R_{π^-} = 100 MeV/c. The broken line to those with R_{π^-} = 80 MeV/c.

perimental points. The X^2 indicates a very satisfactory fit. The points connected by a broken line have been obtained with a pion momentum of 80 MeV/c. The others with a pion momentum of 100 MeV/c.

The Hydrogen data have been normalized using the calculated value (16) of the cross section for single pion photoproduction. These values are probably good to better than 25%.

The results of our linear fits are reported in table II. Y(300) indicates the yield per nucleus calculated at a primary electron energy of 300 MeV from the results of our linear fit. B is the calculated value of the derivative of the yield function. If we neglect the variation of f(E, k) we can write:

$$B(k) = \frac{1}{k}\frac{d^2\sigma(k)}{d\Omega\, dE} \quad \text{nano-barns/steradiant.MeV}^2.$$

In the energy interval of this experiment, (k=400-800) B(k) is constant.

The values for the Li^7 isotope have been calculated from the values for the Li^N and Li^6 targets.

TABLE II

Target	Pion Momentum MeV/c	Pion Charge	B nb/sr.MeV^2	Y μb/sr.MeV
C	80	+	0.241 ± 0.011	0.0967 ± 0.0029
		-	0.251 ± 0.017	0.184 ± 0.0052
C	100	+	0.534 ± 0.017	0.176 ± 0.0045
		-	0.602 ± 0.031	0.307 ± 0.0095
Li^N	100	+	0.313 ± 0.094	0.0951 ± 0.0025
		-	0.443 ± 0.024	0.246 ± 0.0076
Li^6	100	+	0.343 ± 0.017	0.123 ± 0.0048
		-	0.406 ± 0.030	0.199 ± 0.0097
Li^7	100	+	0.305 ± 0.010	0.0914 ± 0.0030
		-	0.438 ± 0.024	0.248 ± 0.0081
H	100	+	0.0307 ± 0.0033	0.0283 ± 0.0012

Table II - indicates the result of the linear fit to our experimental yield curves. As explained in the text Y indicates the calculated value of the yield at E = 300 MeV. B indicates the value of the slopes as obtained from the fit. Associated errors are statistical estimates.

DISCUSSION. -

In a previous measurement[5] of charged pion photoproduction on nuclei it has been shown that the π^- / π^+ ratio is correlated with the mass difference of the isotopes in the final state[7]. In this experiment the π^- / π^+ ratio appeared to be approximately a linear function of this mass difference. This is not true in our case despite the fact that we have used only three different isotopes.

This can be interpreted as a consequence of the fact that in our experiment the energy transfer to the final nucleus is much larger then in the previous one. Therefore we are much less sensitive to nuclear structure effects.

To interpret our results we have assumed that the calculated yields "Y" at 300 MeV are proportional to the single pion photoproduction cross section and that the slopes "B" are proportional to the cross section for double pion photoproduction. Our model then goes as follows:

Single positive pions are photoproduced on protons and are absorbed by the neutrons in the same nucleus. The production is proportional to the total number of protons "Z" in the nucleus. The reabsorption is proportional to the number of neutrons on the nuclear surface ($N^{2/3}$). The cross section is proportional to: $Z/N^{2/3}$.

Single negative pions are photoproduced on neutrons and absorbed by the protons on the surface of the same nucleus. The cross section is proportional to: $N/Z^{2/3}$.

Pion pairs are photoproduced on both nucleons. The absorption of positive pions is then proportional to the number of neutrons on the nuclear surface.

A similar argument holds for negative pions. In conclusion B^+ is proportional to $A/N^{2/3}$; B^- is proportional to $A/Z^{2/3}$.

TABLE III

Target	Y^+	$\frac{Y^+ N^{2/3}}{z}$	Y^-	$\frac{Y^- Z^{2/3}}{N}$	B^+	$\frac{B^+ N^{2/3}}{A}$	B^-	$\frac{B^- Z^{2/3}}{A}$
C	0.176	0.097	0.307	0.172	0.533	0.147	0.601	0.165
Li^7	0.091	0.083	0.248	0.136	0.305	0.118	0.438	0.134
Li^6	0.123	0.088	0.199	0.143	0.343	0.123	0.406	0.145

Table III - compares the experimental results with the hypothesis that we have introduced to explain our data.

ACKNOWLEDGEMENT. -

It is a pleasure to thank Professor Blanc-Lapierre for his hospitality at the Laboratoire de l'Accélérateur Linéaire where this experiment has been performed. We also thank the machine crew headed by L. Burnod, Dr. Buonanni and Dr. Trenta (LNF) for their help with the computer calculations.

REFERENCES AND NOTES. -

(1) - B. Milman, Nuclear Instr. and Meth. 20, 13 (1963).
(2) - R. Bosshard and R. E. Hubert, One Electr. 446, 1 (1964).
(3) - B. Milman, One Electr. 421, 22 (1962).
(4) - W. K. H. Panofsky, Woodard and Yodh, Phys. Rev. 102 1392 (1956).
(5) - R. M. Littauer and D. Walker, Phys. Rev. 86, 838 (1952).
(6) - Ph. Salin, Nuovo Cimento 28, 1294 (1963);
- G. Hohler and Schmidt, Ann. Phys. 28, 34 (1964).
(7) - The mass difference $M_{Z-1} - M_{Z+1}$ is the difference of the ground state masses of the final isobars Z-1 and Z+1 produced by removing or adding one charge to the initial target nucleus.